PCCP

The aromatic pathways of porphins, chlorins and bacteriochlorins†

Jonas Jusélius and Dage Sundholm

Department of Chemistry, PO Box 55 (A.I. Virtasen Aukio 1), FIN-00014, University of Helsinki, Finland. E-mail: jonas@iki.fi, sundholm@chem.helsinki.fi

Received 12th January 2000, Accepted 8th March 2000
Published on the Web 13th April 2000

The aromatic pathways of free-base porphins, chlorins and bacteriochlorins have been studied by calculating the nuclear magnetic shieldings at selected points outside the molecules. The strengths of the induced ring currents for a given magnetic field have been obtained by using the aromatic ring current shieldings (ARCS) method. We found that pyrrolic rings with an inner hydrogen have a local ring current of the same magnitude as the ring current for the pyrrole molecule. The local ring current for pyrrolic rings without an inner hydrogen is between half and one fourth of the pyrrole value depending on the porphyrin. The C_2H_2 units of the pyrrolic rings in free-base porphin have recently been suggested to function as exocyclic bridges, but the present study indicates that this is not the case. The suggested 18π-[16]annulene inner cross aromatic pathway does not exist until all pyrrolic rings are saturated in the β-positions. Free-base *trans*-porphin was found to have the largest ring-current susceptibility among the molecules studied. Porphyrins for which the aromatic pathway has to pass the nitrogen of a pyrrolic unit with an inner hydrogen have significantly smaller ring currents than free-base *trans*-porphin. We also show that the ^{1}H NMR shielding of the inner hydrogens is a sensitive measure of the strength of the ring current for the studied molecules.

I. Introduction

The magnetic shielding of an external magnetic field in the vicinity of an aromatic molecule can be divided into a long-range and a short-range contribution. The short-range contribution is due to the local motion of the electrons around the atoms and in the chemical bonds. The long-range contribution is a result of induced ring currents in the delocalized π-electron system. The short-range shielding vanishes outside the electron density. The shielding due to the induced ring current declines more slowly. This implies that the strength of the ring current of aromatic molecules can be estimated by studying the long-range magnetic shielding function.[1]

Since porphyrins consist of four pyrrole units connected by conjugated bonds to form a larger ring, there are several possible routes for the induced ring current. Traditionally, porphyrins have been considered as a bridged 18π-[18]annulene with the inner NH groups acting as inert bridges.[2–5] Recently, Cyrañski *et al.*[6] studied the aromatic pathway of free-base porphin and concluded that the aromatic pathway of porphins also includes the 18π-[16]annulene internal cross. The 18π-[16]annulene internal cross picture of the porphin molecule implies that the C_2H_2 groups of the pyrrolic rings function only as exocylic bridges. There are, however, other possible routes for the induced ring current in porphyrins. The common denominator for feasible paths is that $(4n + 2)$ π-electrons must be involved.[7,8] For porphyrins, all pathways involving 18, 22, or 26 π-electrons might come into question. The total aromatic pathway may in fact consist of a linear combination of several routes.

The aim of this work is to study the aromatic pathways of porphins, chlorins and bacteriochlorins by performing aromatic ring current shieldings (ARCS),[1] planar aromatic ring current shieldings (PARCS)[1] and nucleus-independent chemical shift (NICS) calculations[9] on different conformations of porphins, chlorins and bacteriochlorins. The ARCS calculations yield the overall current strengths, while the PARCS functions and the NICS values provide information about the fine structure of the currents in multiple-ring systems. Although nuclear magnetic resonance proton shieldings (^{1}H NMR) are usually not an accurate measure of the aromaticity, they can be used to support our interpretations.

The molecules studied were chosen in such a way that they enable us to probe different aspects of the aromaticity of porphyrins. The general idea behind the selection of the molecules was to force the induced ring current to take certain paths. This can be achieved by saturating one or more pyrrolic units at the β-positions. The saturation of the β-carbons effectively prevents the π–π conjugation of the C_β–$C_{\beta'}$ bond in the pyrrolic units. To understand how the induced ring currents flow in porphyrins, the ARCS and PARCS functions as well as NICS values at the ring centers were calculated for a few conformations of porphins, chlorins and bacteriochlorins.

II. Theory

In aromatic molecules an external magnetic field (B_{ext}) induces a ring current (I_{ring}) in the conjugated π-electron system.[10–25] The ring current in turn induces a magnetic field (B_{ind}), which is observed as a long-range magnetic shielding. By assuming that a wire carrying a current is circular and infinitely thin, the Biot-Savart law[26] yields a simple relation between the long-range behavior of the isotropic nuclear magnetic shielding constant σ and the current susceptibility with respect to the applied magnetic field. The final expression for the long-range shielding function with respect to the ring-current susceptibility and to the size of the aromatic pathway then becomes

$$\sigma(z) = -\frac{\mu_0}{2}\frac{\partial I_{ring}}{\partial B_{ext}}\frac{R^2}{(z^2 + R^2)^{3/2}} \quad (1)$$

In eqn. (1), μ_0 is the vacuum permeability, R is the radius of the current loop, $\partial I_{ring}/\partial B_{ext}$ is the current susceptibility, and z

† Dedicated to Professor Reinhart Ahlrichs on the occasion of his 60th birthday.

DOI: 10.1039/b000260g

This journal is © The Owner Societies 2000

is the perpendicular distance from the center of the current loop. In the ARCS approach, the nuclear magnetic shieldings are calculated at discrete points perpendicular to the molecular plane starting from the geometrical center of the current loop. The current susceptibility with respect to the external magnetic field and the current radius can be obtained by fitting the long-range part of the shielding function to eqn. (1). This is done by adjusting the loop radius R until the angular coefficient in the logarithmic representation becomes $\frac{3}{2}$. The current derivative can then be deduced from the intercept. The strength of the induced ring current (I_{ring}) for a given magnetic field (B_{ext}) is obtained from the current susceptibility as

$$I_{\text{ring}} = \frac{\partial I_{\text{ring}}}{\partial B_{\text{ext}}} B_{\text{ext}} \tag{2}$$

In the PARCS approach, the shielding function is calculated in a plane parallel to the molecular plane at a certain distance from it. In this work, we chose a distance of 7 a_0 from the molecular plane, since at that distance the electron density is negligible and the shielding is only due to the induced currents in the molecule. As seen in eqn. (1), the larger the current radius, the more long-range is the induced shielding.

The PARCS data provide some information about anisotropies in the ring currents, but they do not directly yield any information about the fine structure of the currents. It is, however, possible to manipulate the PARCS data in order to get more detailed information about current paths. The calculated two-dimensional PARCS functions can be expanded in two-dimensional momentum functions analogously to the expansion in spherical harmonics in the three-dimensional case

$$\varphi(r, \theta) = \sum_i f_i(r)\chi_i(\theta), \tag{3}$$

where $\chi_i(\theta)$ are angular functions, *i.e.* s, p_x, p_y, $d_{x^2-y^2}$ and d_{xy}, while $f_i(r)$ are the corresponding radial parts. The radial functions for the first few angular functions can be obtained by numerical integration and Gram–Schmidt orthogonalization. The projected PARCS functions are obtained as

$$\tilde{\varphi}(r, \theta) = \varphi(r, \theta) - \sum_k \frac{\int \chi_k(\theta)\varphi(r, \theta)\, \mathrm{d}\theta}{\int \chi_k^2(\theta)\, \mathrm{d}\theta} \chi_k(\theta) \tag{4}$$

By projecting out the dominating s term and eventually some of the higher-order terms from the two-dimensional PARCS function, the underlying fine structure of the ring current is revealed.

III. Computational methods

The molecular structures have been optimized as the resolution-of-the-identity density-functional theory (RI-DFT) level[27] using the Becke–Perdew (B-P) parameterization[28–30] as implemented in TURBOMOLE.[31] The nuclear magnetic shieldings have been calculated at Hartree–Fock self-consistent field (SCF) level.[32,33] To ensure origin independence in the shielding calculations, the gauge-including-atomic-orbital (GIAO) approach has been employed.[11,34–36] In the structure optimization, the Karlsruhe split-valence basis sets[37] augmented with polarization functions on C and N[38] were employed [SV(P)], while in the shielding calculations the basis set was further augmented with polarization functions on H (SVP).

IV. Results

The nuclear magnetic shieldings have been studied for the following free-base porphins and chlorins: *trans*-porphin (t-PH_2), *cis*-porphin (c-PH_2), *trans*-chlorin (t-$CH_2^{(a)}$ and t-$CH_2^{(b)}$ and *cis*-chlorin (c-$CH_2^{(a)}$ and c-$CH_2^{(b)}$). The t-$CH_2^{(a)}$ and c-$CH_2^{(a)}$ molecules do not have any inner hydrogens connected to the pyrrolic ring saturated in the β-positions, while t-$CH_2^{(b)}$ and c-$CH_2^{(b)}$ have one inner hydrogen connected to the β-saturated ring. The molecular structures of the porphins and the chlorins are shown[39] in Figs. 1 and 2.

Four bacteriochlorins were also considered. One of the *trans*-bacteriochlorins (t-$BCH_2^{(a)}$) has the β-saturated pyrrolic rings in *trans* position, but it does not have any inner hydrogen connected to the β-saturated rings. The other *trans*-bacteriochlorin (t-$BCH_2^{(b)}$) considered has the β-saturated pyrrolic rings in *trans* position and the inner hydrogens are connected to the β-saturated rings. *trans*-Isobacteriochlorin (t-$IBCH_2$) has the β-saturated pyrrolic rings in *cis* position and the inner hydrogens in *trans* position. *cis*-Bacteriochlorin (c-BCH_2) has the β-saturated rings in *trans* position, while the inner hydrogens are *cis*. Both t-$IBCH_2$ and c-BCH_2 have one inner hydrogen connected to a β-saturated ring. The molecular structures of the bacteriochlorins are shown in Fig. 3.

The porphyrins denoted t-$3BCH_2$ have three β-saturated pyrrolic rings and the inner hydrogens are in *trans* position. For t-$3BCH_2^{(a)}$, one inner hydrogen is connected to the unsaturated ring; while for t-$3BCH_2^{(b)}$, both hydrogens are connected to the β-saturated rings. The t-$4BCH_2$ molecule has all four pyrrolic rings saturated in the β-positions and the inner hydrogen in *trans* position. For the t-$PH_2^{(m)}$ molecule, all the *meso* carbons are saturated. The structures of t-$3BCH_2^{(a)}$, t-$3BCH_2^{(b)}$, t-$4BCH_2$ and t-$PH_2^{(m)}$ are shown in Fig. 4. The ^{1}H

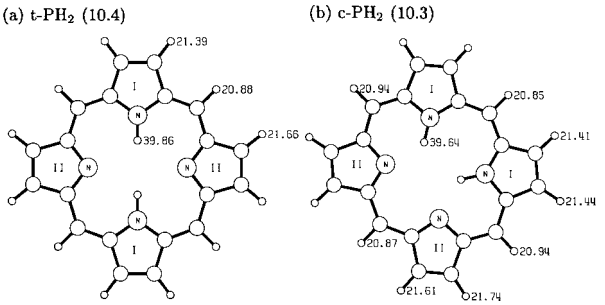

Fig. 1 The molecular structures of the porphins, their ^{1}H NMR shieldings (in ppm) and current susceptibilities (in nA T^{-1}).

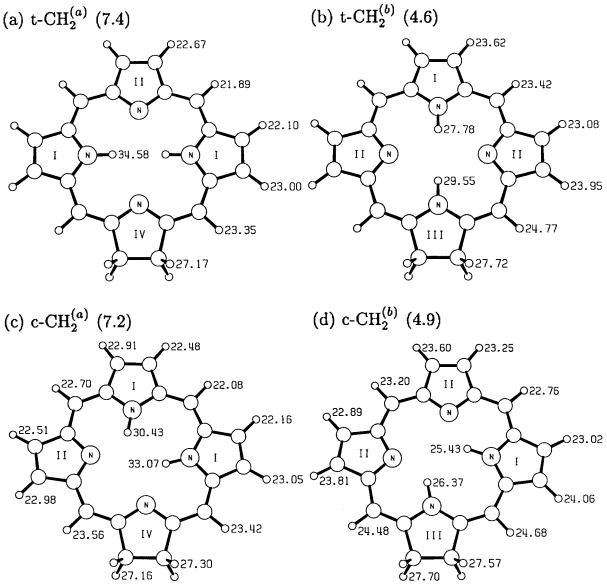

Fig. 2 The molecular structures of the chlorins, their ^{1}H NMR shieldings (in ppm) and current susceptibilities (in nA T^{-1}).

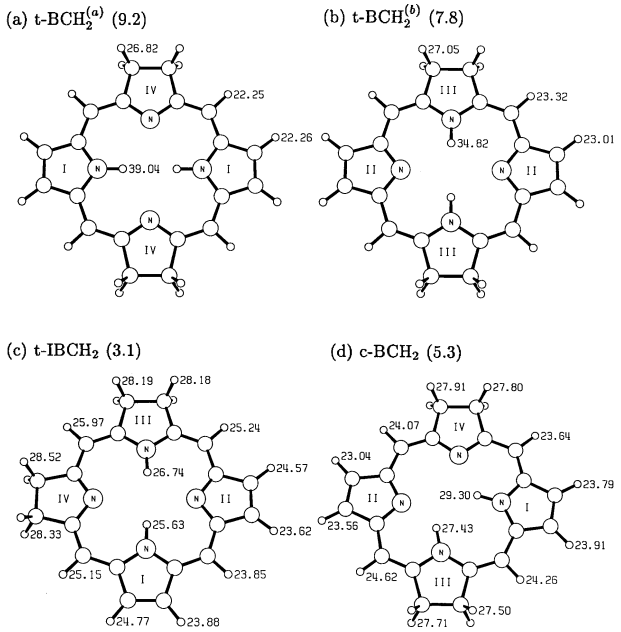

Fig. 3 The molecular structures of the bacteriochlorins, their ^{1}H NMR shieldings (in ppm) and current susceptibilities (in nA T^{-1}).

NMR shieldings are also given in Figs. 1–4. The optimized molecular structures can be downloaded from our World-Wide-Web (www) server.[40]

The current susceptibilities have been obtained from the long-range magnetic shieldings as described in the previous section. In Fig. 5, the ARCS plots for the strongly aromatic t-PH$_2$ molecule and the less aromatic t-3BCH$_2^{(a)}$ molecule are shown. The abscissa (z) is the distance (in a_0) from the center of the porphyrin nucleus, while the ordinate is the calculated shielding function (σ in ppm). As seen in Fig. 5, there is a perfect agreement between the calculated shieldings and the line fitted to the Biot-Savart law. The intercepts correspond to current strengths of 10.4 and 2.5 nA for t-PH$_2$ and t-3BCH$_2^{(a)}$, respectively, when the applied magnetic field is 1 T. Judged from the current strengths, one may claim that t-PH$_2$ is four times more aromatic than t-3BCH$_2^{(b)}$. Actually, one may question whether t-3BCH$_2^{(b)}$ can be considered aromatic. The

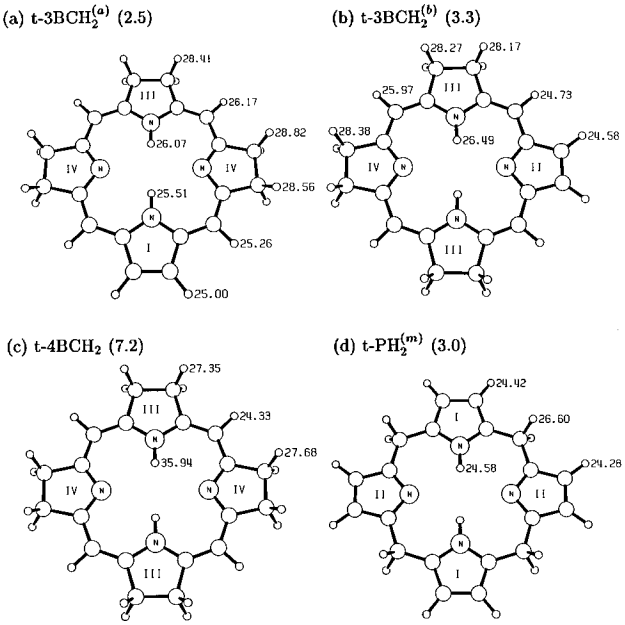

Fig. 4 The molecular structures of t-3BCH$_2^{(a)}$, t-3BCH$_2^{(b)}$, t-4BCH$_2$ and t-PH$_2^{(m)}$, their ^{1}H NMR shieldings (in ppm) and current susceptibilities (in nA T^{-1}).

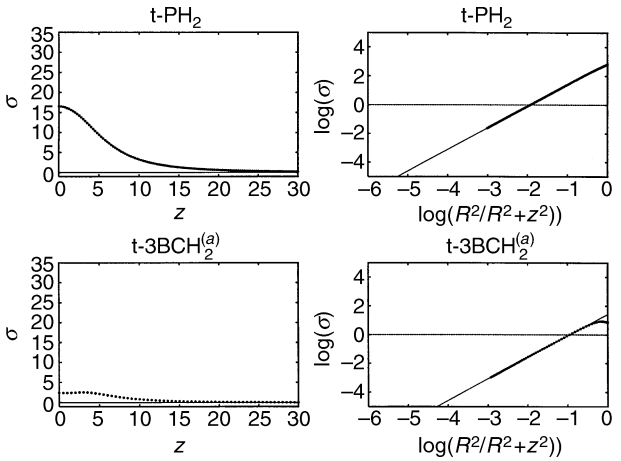

Fig. 5 The calculated ARCS functions (in ppm) for t-PH$_2$ and t-3BCH$_2^{(a)}$ as well as the logarithmic fit of the ARCS functions to eqn. (1).

ARCS plots for the other molecules are very similar and they can be obtained from our World-Wide-Web (www) server.[40]

The ring-current susceptibility (in nA T^{-1}) and the corresponding current radius (in a_0) for the studied molecules are summarized in Table 1. The largest ring-current susceptibilities were obtained for the two porphin molecules. In general, the calculated current radii are larger than the geometrical radii. The only exception is t-4BCH$_2$. The reason for this is that the geometric radii have been estimated from the distances between the *meso* carbons. The current susceptibility of 10.4 nA T^{-1} for the porphins is of the same magnitude as for the pyrrole molecule. Other porphyrins with high current susceptibilities are t-CH$_2^{(a)}$, c-CH$_2^{(a)}$, t-BCH$_2^{(a)}$, t-BCH$_2^{(b)}$ and t-4BCH$_2$. The first three of these molecules have no inner hydrogens connected to the β-saturated ring.

In Table 2, the total energies (in E_h) of the studied molecules are given. The energy differences (in kJ mol^{-1}) between the different conformations are also given. The *trans* conformations are lower in energy than the *cis* ones. The conformations that have no inner hydrogens connected to the β-saturated rings are energetically lower than the other conformations. In the last column, the hydrogenation energies (in kJ mol^{-1}) are compared to the energy gain when t-PH$_2$ is hydrated yielding t-CH$_2^{(a)}$. As seen in Table 2, the hydrogenation energy becomes smaller for each H$_2$ added to the

Table 1 The geometrical ring radius (in a_0), the effective ring radius of the ring current (in a_0) and the induced ring-current susceptibility (in nA T^{-1})

Molecule[a]	Geometric radius	Current radius	$\partial I_{ring}/\partial B$
t-PH$_2$	5.88–6.54	6.84	10.4
c-PH$_2$	5.89–6.53	6.83	10.3
t-CH$_2^{(a)}$	5.89–6.54	6.87	7.4
t-CH$_2^{(b)}$	5.89–6.54	7.24	4.6
c-CH$_2^{(a)}$	5.89–6.53	6.86	7.2
c-CH$_2^{(b)}$	5.89–6.53	7.18	4.9
t-BCH$_2^{(a)}$	5.89–6.55	6.44	9.2
t-BCH$_2^{(b)}$	5.92–6.58	6.38	7.8
t-IBCH$_2$	5.89–6.54	7.36	3.1
c-BCH$_2$	5.89–6.53	6.74	5.3
t-3BCH$_2^{(a)}$	5.90–6.55	7.12	2.5
t-3BCH$_2^{(b)}$	5.89–6.54	6.80	3.3
t-4BCH$_2$	5.90–6.55	5.68	7.2
t-PH$_2^{(m)}$	6.08–6.76	8.64	3.0
Pyrrole	2.10–2.24	1.60	10.5

[a] t-CH$_2^{(a)}$, t-BCH$_2^{(a)}$ and c-CH$_2^{(a)}$ do not have any inner hydrogen connected to the β-saturated pyrrolic rings.

Table 2 The total energy of the studied porphyrins (in E_h), the energy differences between different conformations (in kJ mol^{-1}), the hydrogenation energies (in E_h) and the differences in hydrogenation energies (in kJ mol^{-1}) relative to the hydrogenation of t-PH_2 to t-$CH_2^{(a)}$

Molecule	E_{total}	$\Delta E_{Conf.}$	$E_{Hydr.}$	$\Delta E_{Hydr.}$
t-PH_2	−988.892 216	—	—	—
c-PH_2	−988.881 559	28.0	—	—
t-$CH_2^{(a)}$	−990.099 631	—	1.207 415	—
t-$CH_2^{(b)}$	−990.087 614	31.6	—	—
c-$CH_2^{(a)}$	−990.089 289	27.2	—	—
c-$CH_2^{(b)}$	−990.077 083	59.2	—	—
t-$BCH_2^{(a)}$	−991.303 147	—	2.410 931	10.2
t-$BCH_2^{(b)}$	−991.276 420	70.2	—	—
t-$IBCH_2$	−991.293 349	25.7	—	—
c-BCH_2	−991.281 122	57.8	—	—
t-$3BCH_2^{(a)}$	−992.493 553	—	3.601 337	44.7
t-$3BCH_2^{(b)}$	−992.478 396	39.8	—	—
t-$4BCH_2$	−993.670 782	—	4.778 566	79.3
t-$PH_2^{(m)}$	−991.186 082	—	2.293 866	—

molecules. This results in a stabilization order of t-PH_2 > t-$CH_2^{(a)}$ > t-$BCH_2^{(a)}$ > t-$3BCH_2^{(a)}$ > t-$4BCH_2$.

The ^{1}H NMR shieldings of the inner hydrogens correlate well with the current susceptibility obtained from the ARCS calculations. In Fig. 6, the ^{1}H NMR shieldings of the hydrogens connected to the β-unsaturated pyrrolic rings are compared to the obtained current susceptibilities. Exceptions are

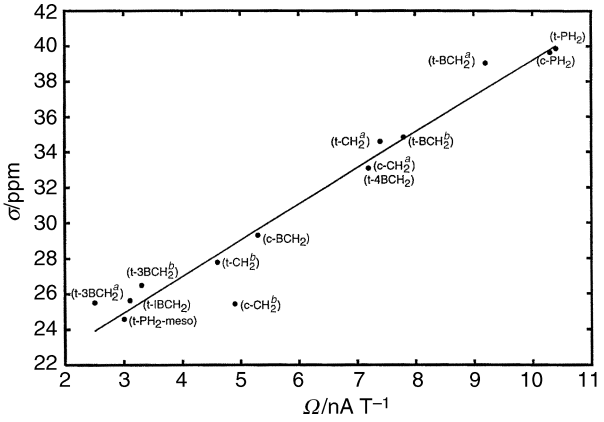

Fig. 6 The calculated ^{1}H NMR shieldings (σ in ppm) for the inner hydrogens as compared to the calculated ring-current susceptibilities (Ω in nA T^{-1}).

Table 3 The relative aromaticity of the studied porphyrins in comparison to benzene

Molecule	Ring current[a]	ARCS index	NICS index
Pyrrole	10.5	1.31	1.49
t-PH_2	10.4	1.30	1.54
c-PH_2	10.3	1.29	1.53
t-$BCH_2^{(a)}$	9.2	1.15	1.40
Benzene	**8.0**	**1.00**	**1.00**
t-$BCH_2^{(b)}$	7.8	0.98	1.20
t-$CH_2^{(a)}$	7.4	0.93	1.05
c-$CH_2^{(a)}$	7.2	0.90	1.01
t-$4BCH_2$	7.2	0.89	1.13
c-BCH_2	5.3	0.67	0.72
c-$CH_2^{(b)}$	4.9	0.61	0.60
t-$CH_2^{(b)}$	4.6	0.58	0.56
t-$3BCH_2^{(b)}$	3.3	0.41	0.38
t-$IBCH_2$	3.1	0.39	0.31
t-$PH_2^{(m)}$	3.0	0.38	0.19
t-$3BCH_2^{(a)}$	2.5	0.31	0.23

[a] In nA for B_{ext} = 1 T.

t-$BCH_2^{(b)}$, t-$3BCH_2$ and t-$4BCH_2$ which do not have any inner hydrogens connected to β-unsaturated rings. The largest discrepancy of about 3 ppm is obtained for c-$CH_2^{(b)}$.

In Table 3, the ARCS aromaticity indices deduced from the ring-current susceptibilities are compared to the NICS aromaticity indices. The NICS index is defined as the NICS value relative to the NICS value for benzene. Note that the sign convention for the NICS values differs from that introduced by Schleyer *et al.*[9] There is a qualitative agreement between the two aromaticity indices. In comparison with the ARCS indices, the NICS values seem to overestimate the aromaticity of pyrrole and the porphyrins.

V. The aromatic pathways

A. Porphins

The ARCS and NICS calculations on chlorins show that, when a pyrrolic ring lies outside the current pathway, it has negative shielding constants at the ring center. Since all NICS values for the porphins are positive (see Table 4), the C_2H_2 units cannot be considered to be exocyclic bridges but they participate in the aromatic pathway. Pyrrolic rings with a hydrogen have NICS values of the same magnitude as for the pyrrole molecule.

As seen in Fig. 7, the projected PARCS function has local maxima above each pyrrolic ring indicating the presence of local ring currents in the pyrrolic rings. For the pyrrolic rings without an inner hydrogen, the maximum is significantly smaller, reflecting a weaker current circulating in these rings. Fig. 7(a) shows the full PARCS function for t-PH_2, while in Fig. 7(b), the circular symmetric part (the s part) has been projected out.

The proton shieldings of the β-hydrogens also indicate that pyrrolic rings with an inner hydrogen have a stronger local current than the two other pyrrolic rings. Ligabue *et al.*[24] showed recently that in aromatic hydrocarbons such as triphenylene the individual benzene rings must be considered to have local ring currents.

For aromatic systems, $(4n + 2)$ π-electrons are involved in the aromatic pathway. For porphins, this means that all paths involving 18, 22, or 26 π-electrons may come into question. The total aromatic pathway can also be a superposition of

Table 4 The nuclear-independent chemical shift (NICS) values (in ppm) calculated at the center of the pyrrolic rings[a] and at the center of the porphyrin nucleus

Molecule	Ring I	Ring II	Ring III	Ring IV	Center
t-PH_2	15.46	4.71	—	—	16.52
c-PH_2	15.49	4.50	—	—	16.38
t-$CH_2^{(a)}$	13.63	8.61	—	−5.90	11.21
t-$CH_2^{(b)}$	14.86	4.64	−1.99	—	5.98
c-$CH_2^{(a)}$	15.85[b]	2.81	—	−5.69	10.80
c-$CH_2^{(b)}$	13.40	7.81[c]	−2.31	—	6.40
t-$BCH_2^{(a)}$	16.97	—	—	−7.36	14.99
t-$BCH_2^{(b)}$	—	7.51	−5.79	—	12.86
t-$IBCH_2$	13.76	7.45	−0.32	−2.02	3.33
c-BCH_2	17.03	3.39	−2.76	−3.95	7.68
t-$3BCH_2^{(a)}$	15.14	—	0.49	−1.36	2.41
t-$3BCH_2^{(b)}$	—	12.84	−0.91	−2.15	4.09
t-$4BCH_2$	—	—	−4.87	−5.30	12.10
t-$PH_2^{(m)}$	16.18	1.06	—	—	1.98
Pyrrole	—	—	—	—	15.91

[a] Ring I is unsaturated in the β-position and has an inner hydrogen. Ring II is unsaturated in the β-position and has no inner hydrogen. Ring III is saturated in the β-position and has an inner hydrogen. Ring IV is saturated in the β-position and has no inner hydrogen. [b] The NICS value for the ring neighbour to the β-saturated pyrrolic ring is 14.02 ppm. [c] The NICS value for the ring neighbour to the β-saturated pyrrolic ring is 5.20 ppm.

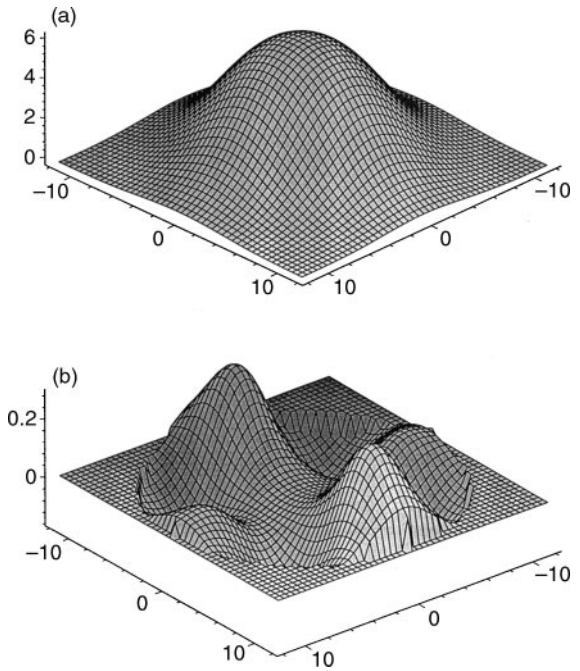

Fig. 7 (a) The nuclear magnetic shieldings for free-base porphin (t-PH_2) calculated at a distance of 7 a_0 from the molecular plane. (b) The PARCS function after the circular symmetric part has been projected out.

several paths. A pyrrolic ring with an inner hydrogen is aromatic and contributes six π-electrons to the aromatic pathway. A pyrrolic ring without an inner hydrogen contributes five π-electrons. The *meso* carbon bridges contribute a total of four π-electrons. For a pyrrolic ring with an inner hydrogen, both the inner and the outer route contribute four π-electrons. For a pyrrolic ring without an inner hydrogen, the inner route involves three π-electrons and the outer route involves four π-electrons. Thus for porphins, one 26π-electron path, three symmetrically unique 22π-electron paths, and two 18π-electron paths can be constructed.

Since all pyrrolic rings in free-base porphin have local ring currents which are an integrated part of the conjugated π-electron system, all 26π-electrons must be considered to belong to the aromatic pathway. The current strength for pyrrolic rings without an inner hydrogen is about four times weaker than for the pyrrolic rings with an inner hydrogen. This implies that porphins must have significant 22π-electron contributions to the total aromatic pathway. The most important 22π-electron path consists of two aromatic pyrrolic rings with an inner hydrogen, four *meso* carbons and the inner route at the two other pyrrolic rings. Two 18π-electron paths might also contribute to the aromatic pathway. Cyrañski *et al.*[16] suggested that the aromatic pathway of porphins includes the 18π-[16]annulene internal cross. If only the 18π-[16]annulene internal cross current path were present, the whole area outside the current path in the molecular plane should be deshielded. This would imply that all the centers of the pyrrolic rings outside the current loop have negative shieldings at the ring centers (NICS values). Since this is not the case, it is unlikely that the 18π-[16]annulene internal cross is of importance for porphins.

The traditional 18π-[18]annulene aromatic pathway consists of the outer path at the pyrrolic rings with an inner hydrogen, and the inner path at the pyrrolic rings without an inner hydrogen. Since the pyrrolic rings with an inner hydrogen have local ring currents which are of the same magnitude as for the pyrrole molecule, it is unlikely that the traditional 18π-[18]annulene path is the dominating contribution to the total aromatic pathway of porphins. The present study indicates that the aromatic pathway of porphins must be considered to be a superposition of several $(4n + 2)\pi$ paths, of which the dominating contributions are the 22π- and 26π-electron paths. The 18π-[16]annulene internal cross pathway, the traditional 18π-[18]annulene pathway, the most important 22π-electron pathway and the 26π-electron aromatic pathway for t-PH_2 are sketched in Fig. 8.

B. Chlorins

Chlorins are porphyrins with one β-saturated pyrrolic ring destroying the π-conjugation at the β-carbons. The saturation of the β-carbons effectively prevents the ring current from taking the outer route at that particular pyrrolic unit. Since chlorins have 24π-electrons, all π-electrons cannot directly participate in the aromatic pathway. However, when one considers the aromatic pathway to be a superposition of several 22π-electron paths, all 24π-electrons can form the total aromatic pathway. For chlorins, pyrrolic rings with an inner hydrogen have strong local ring currents. For t-$CH_2^{(a)}$ and c-$CH_2^{(b)}$, the pyrrolic ring without an inner hydrogen has a NICS values which is twice as large as for the corresponding unit in t-PH_2, indicating a stronger local ring current (see Table 4). This can be explained by assuming that the aromatic pathway consists of a superposition of two 22π-electron pathways. In t-$CH_2^{(a)}$, for example, the two 22π-electron routes consist of six π-electrons from one aromatic pyrrolic ring with an inner hydrogen, five π-electrons from the pyrrolic ring without an inner hydrogen, four π-electrons from the *meso* carbons, four π-electrons from the outer path of the other pyrrolic ring with an inner hydrogen, and three π-electrons from the inner path of the β-saturated pyrrolic ring. Another 22π-electron path consists of the two pyrrolic rings with an inner hydrogen, and the inner paths at the two other pyrrolic rings. For c-CH_2, the NICS value for the pyrrolic ring without an inner hydrogen is only 2.8 ppm, indicating that the inner paths at the pyrrolic rings without an inner hydrogen is the dominating one. For the chlorins with an inner hydrogen connected to the β-saturated ring, the ring current is significantly weaker than for the other chlorins. For t-$CH_2^{(a)}$ and c-$CH_2^{(a)}$, the obtained current susceptibilities are 7.4 and 7.2 nA T^{-1}, respectively, while for the two other chlorins the corresponding values are 4.6 and 4.9 nA T^{-1}.

C. Bacteriochlorins

Bacteriochlorins have 22π-electrons and consist of four pyrrolic rings of which two are β-saturated. The two *trans*-

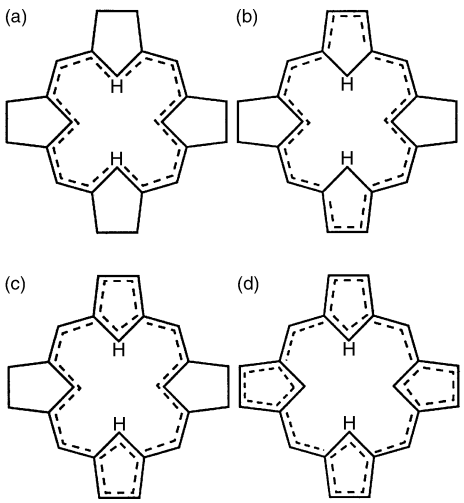

Fig. 8 (a) The 18π-[16]annulene internal cross pathway, (b) the traditional 18π-[18]annulene pathway, (c) the most important 22π-electron pathway and (d) the 26π-electron aromatic pathway for t-PH_2.

bacteriochlorins have large current susceptibilities, while the current susceptibility for c-BCH_2 and t-$IBCH_2$ is 5.3 and 3.1 nA T^{-1}, respectively. The aromatic pathway for t-$BCH_2^{(a)}$ consists of two aromatic pyrrolic rings with an inner hydrogen and the inner path at the β-saturated rings yielding a 22π-electron pathway. For t-$BCH_2^{(b)}$, the pyrrolic rings without an inner hydrogen have large local ring currents. The aromatic pathway for t-$BCH_2^{(b)}$ consists of the two aromatic pyrrolic rings without an inner hydrogen and the inner paths at the β-saturated rings. Since for t-$BCH_2^{(b)}$, the current must pass two inner hydrogens the ring-current susceptibility is 7.8 nA T^{-1} as compared to 9.2 nA T^{-1} for t-$BCH_2^{(a)}$. t-$BCH_2^{(a)}$ has current susceptibility almost as large as t-PH_2. It is questionable whether t-$IBCH_2$ with a current susceptibility of 3.1 nA T^{-1} can be considered aromatic.

D. t-3BCH_2, t-4BCH_2 and t-$PH_2^{(m)}$

The t-3BCH_2 molecules have three β-saturated pyrrolic rings yielding 20 π-electrons. The only possible current pathway consisting of $(4n + 2)$ π-electrons is the 18π-[16]annulene inner cross path. The current susceptibilities for the studied t-3BCH_2 molecules are only 2.5 and 3.3 nA T^{-1}, respectively, which indicates that they are not particularly aromatic. Energetically, t-3$BCH_2^{(a)}$ lies lower than t-3$BCH_2^{(b)}$, since the unsaturated pyrrolic ring with an inner hydrogen is much more aromatic than the pyrrolic ring without the inner hydrogen. Hence, t-3$BCH_2^{(a)}$ is more stable than t-3$BCH_2^{(b)}$, which does not have any inner hydrogen connected to the β-saturated ring. The t-3BCH_2 molecules do not have a significant 18π-[16]annulene inner cross aromatic pathway.

The current susceptibility of t-4BCH_2 of 7.2 nA T^{-1} is of the same size as for t-$CH_2^{(a)}$ and c-$CH_2^{(a)}$. For t-4BCH_2, the only possible aromatic pathway is the 18π-annulene inner cross path. As expected, t-4BCH_2 has a smaller ring-current radius than the other porphyrins studied. t-4BCH_2 is also the only molecule among the studied ones which has a significant 18π-[16]annulene inner cross aromatic pathway. The reason is that the porphyrins in general are stabilized by the local aromaticity of the pyrrolic rings, and their aromaticity would be weakened by the 18π-[16]annulene pathway. In t-4BCH_2, all pyrrolic rings are non-aromatic and the 18π-[16]annulene aromatic pathway stabilizes the molecule energetically.

In Table 2, it can be seen that t-4BCH_2 is the most destabilized molecule as compared to the other porphyrins. Even though t-4BCH_2 has a relatively strong ring current, it lies energetically high. The hydrogenation energy is 79.3 kJ mol^{-1} larger when two hydrogens are added to t-3$BCH_2^{(a)}$ than when two hydrogens are added to t-PH_2 yielding t-$CH_2^{(a)}$. The general trend for the hydrogenation of the β-carbons for the porphyrins is that the energy gain decreases with the number of β-saturated rings.

The t-$PH_2^{(m)}$ molecule has a very large current radius, since the two pyrrolic rings with an inner hydrogen simulate a global ring current. The saturated *meso* carbons prevent the global ring current, which is also reflected on the ARCS value. From the NICS values in Table 4 one can see that the rings without an inner hydrogen are not particularly aromatic, which indicates that the pyrrolic rings without an inner hydrogen need the conjugated π-electron environment in order to sustain a local ring current. The obtained current susceptibility for t-$PH_2^{(m)}$ is 3.0 nA T^{-1}, which shows that the contribution from the pyrrolic rings to the ARCS values of the porphyrins is in general much smaller than the contribution from the porphyrin loop.

VI. Summary

The present study shows that the total aromatic pathway of porphyrins must be considered as a superposition of several pathways. For porphin, all 26π-electrons are part of the aromatic pathway. The pathway must be considered mainly as a superposition of the 26π-electron path and two 22π-electron paths. For chlorins, all 24π-electrons participate in the aromatic pathway, which implies that the total aromatic pathway must be considered to consist of a superposition of 22π-electron paths. For bacteriochlorins, all 22π-electrons are involved in the aromatic pathway.

The β-unsaturated pyrrolic rings in porphyrins have local ring currents which are intergraded parts of the total aromatic pathway. The current strength of the pyrrolic rings with an inner hydrogen is of about the same size as for the free pyrrole molecule. Pyrrole rings without an inner hydrogen have significantly smaller local ring currents than the rings with an inner hydrogen. The porphyrins are energetically stabilized by the aromaticity of the pyrrolic rings.

The 18π-[16]annulene inner cross aromatic pathway does not exist in porphyrins until all pyrrolic rings are non-aromatic. This means that the C_2H_2 units of the pyrrolic rings do not function as exocyclic bridges. We also found that the ^1H NMR shieldings of the inner hydrogens correlate well with the calculated current susceptibilities, and thus can be used as an experimental measure for the aromaticity of free-base porphyrins.

Acknowledgements

All calculations have been performed with the TURBOMOLE program package which has been developed in Karlsruhe under the supervision of Prof. Reinhart Ahlrichs. The generous support by Prof. P. Pyykkö and by The Academy of Finland is also acknowledged. All calculations have been done on a PC equipped with the LINUX operating system.

References

1 J. Jusélius and D. Sundholm, *Phys. Chem. Chem. Phys.*, 1999, **1**, 3429.
2 E. Vogel, W. Haas, B. Knipp, J. Lex and H. Schmickler, *Angew. Chem. Int. Ed. Engl.*, 1988, **27**, 406.
3 E. Vogel, *J. Heterocycl. Chem.*, 1996, **33**, 1461.
4 T. D. Lash and S. T. Chaney, *Chem. Eur. J.*, 1996, **2**, 944.
5 T. D. Lash, J. L. Romanic, J. Hayes and J. D. Spence, *Chem. Commun.*, 1999, 819.
6 M. K. Cyrañski, T. M. Krygowski, M. Wisiorowski, N. J. R. van Eikema Hommes and P. von Ragué Schleyer, *Angew. Chem. Int. Ed. Engl.*, 1998, **37**, 177.
7 D. Lloyd, *J. Chem. Inf. Comput. Sci.*, 1996, **36**, 442.
8 P. von Ragué Schleyer and H. Jiao, *Pure Appl. Chem.*, 1996, **28**, 209.
9 P. von Ragué Schleyer, C. Maerker, A. Dransfeld, H. Jiao and N. J. R. van Eikema Hommes, *J. Am. Chem. Soc.*, 1996, **118**, 6317.
10 L. Pauling, *J. Chem. Phys.*, 1936, **4**, 637.
11 F. London, *J. Phys. Radium*, 1937, **8**, 397.
12 J. A. Pople, *J. Chem. Phys.*, 1956, **24**, 1111.
13 J. A. Pople, *Mol. Phys.*, 1958, **1**, 175.
14 R. McWeeny, *Mol. Phys.*, 1958, **1**, 311.
15 J. A. Elvidge and L. M. Jackman, *J. Chem. Soc.*, 1961, 859.
16 R. J. Abraham, R. C. Sheppard, W. A. Thomas and S. Turner, *Chem. Commun.*, 1965, 43.
17 W. Kutzelnigg, C. van Wüllen, U. Fleischer, R. Franke and T. v. Mourik, in *Nuclear Magnetic Shieldings and Molecular Structure*, ed. J. A. Tossell, Kluwer Academic, Dordrecht, 1993, pp. 141–161.
18 V. I. Minkin, M. N. Glukhovtsev and B. Y. Simkin, *Aromaticity and Antiaromaticity—Electronic and Structural Aspects*, Wiley, New York, 1994.
19 U. Fleischer, W. Kutzelnigg, P. Lazzeretti and V. Mühlenkamp, *J. Am. Chem. Soc.*, 1994, **116**, 5298.
20 M. Bilde and A. Hansen, *Mol. Phys.*, 1997, **92**, 237.
21 I. Černušak, P. W. Fowler and E. Steiner, *Mol. Phys.*, 1997, **91**, 401.
22 R. Zanasi and P. Lazzeretti, *Mol. Phys.*, 1997, **92**, 609.
23 D. B. Chesnut, *J. Chem. Phys.*, 1998, **231**, 1.
24 A. Ligabue, U. Pincelli, P. Lazzeretti and R. Zanasi, *J. Am. Chem. Soc.*, 1999, **121**, 5513.

25 I. Morao and F. P. Cossío, *J. Org. Chem.*, 1999, **64**, 1868.
26 G. Arfken, *Mathematical Methods for Physicists*, Academic Press, Orlando, 1985.
27 K. Eichkorn, O. Treutler, H. Öhm, M. Häser and R. Ahlrichs, *Chem. Phys. Lett.*, 1995, **240**, 283.
28 S. H. Vosko, L. Wilk and M. Nusair, *Can. J. Phys.*, 1980, **58**, 1200.
29 J. P. Perdew, *Phys. Rev. B*, 1986, **33**, 8822.
30 A. D. Becke, *Phys. Rev. B*, 1988, **38**, 3098.
31 R. Ahlrichs, M. Bär, M. Häser, H. Horn and C. Kölmel, *Chem. Phys. Lett.*, 1989, **162**, 165.
32 M. Häser, R. Ahlrichs, H. P. Baron, P. Weis and H. Horn, *Theor. Chim. Acta*, 1992, **83**, 551.
33 M. Kollwitz, M. Häser and J. Gauss, *J. Chem. Phys.*, 1998, **108**, 8295.
34 H. Hameka, *Mol. Phys.*, 1958, **1**, 203.
35 R. Ditchfield, *Mol. Phys.*, 1974, **27**, 789.
36 K. Wolinski, J. F. Hinton and P. Pulay, *J. Am. Chem. Soc.*, 1990, **112**, 8251.
37 A. Schäfer, H. Horn and R. Ahlrichs, *J. Chem. Phys.*, 1992, **97**, 2571.
38 T. H. Dunning, Jr., *J. Chem. Phys.*, 1989, **90**, 1007.
39 M. N. Burnett and C. K. Johnson, *ORTEP-III: Oak Ridge Thermal Ellipsoid Plot Program for Crystal Structure Illustrations*, Tech. Rep. ORNL-6895, Oak Ridge National Laboratory, 1996.
40 http://www.chem.helsinki.fi/ ~ sundholm/qc/porphin_arcs